

Kinetics of Chromium(III) Oxidation by Manganese(IV) Oxides Using Quick Scanning X-ray Absorption Fine Structure Spectroscopy (Q-XAFS)

GAUTIER LANDROT,*
MATTHEW GINDER-VOGEL, AND
DONALD L. SPARKS

Department of Plant and Soil Science and Delaware
Environmental Institute, University of Delaware, 152
Townsend Hall, Newark, Delaware 19716

Received June 15, 2009. Revised manuscript received
October 28, 2009. Accepted October 31, 2009.

The initial kinetics of Cr(III) oxidation on mineral surfaces is poorly understood, yet a significant portion of the oxidation process occurs during the first seconds of reaction. In this study, the initial rates of Cr(III) oxidation on hydrous manganese oxide (HMO) were measured at three different pH values (pH 2.5, 3, and 3.5), using a quick X-ray absorption fine structure spectroscopy (Q-XAFS) batch method. The calculated rate constants were 0.201, 0.242, and 0.322 s⁻¹ at pH 2.5, 3, and 3.5, respectively. These values were independent of both [Cr(III)] and [Mn(II)] and mixing speed, suggesting that the reaction was “chemically” controlled and not dependent upon diffusion at the time period the rate parameters were measured. A second-order overall rate was found at three pH values. This represents the first study to determine the *chemical* kinetics of Cr(III) oxidation on Mn-oxides. The results have important implications for the determination of rapid, environmentally important reactions that cannot be measured with traditional batch and flow techniques. An understanding of these reactions is critical to predicting the fate of contaminants in aquatic and terrestrial environments.

Introduction

Kinetics of geochemical processes range over time scales of seconds to millennia (1). For example, we know that certain ion exchange, redox, and sorption processes can occur on second or faster time scales. However, some sorption processes, particularly those involving organic chemicals, may continue for periods of days and weeks before steady state is attained. Many geochemical processes are characterized by a biphasic process, a rapid reaction occurring over minutes and hours, followed by a slower reaction that continues for hours, and perhaps days. However, for ion exchange, electron transfer, and adsorption reactions, a major portion of the total reaction process often occurs on time scales of minutes with a significant part of the initial reaction having occurred before the first data point is collected using traditional batch and flow techniques. Few studies have appeared in the geochemistry literature where these rapid initial reaction rates have been measured. An electron

paramagnetic resonance spectroscopy stopped-flow (EPR-SF) technique was used (2) to measure millisecond reaction rates of Mn²⁺ on MnO₂. While this is a useful technique, it is limited to the measurement of paramagnetic elements. Chemical relaxation techniques, especially pressure-jump relaxation, have been employed to study rapid sorption processes on metal oxides. However, the kinetic rate constants are indirectly determined via linearized rate equations that are dependent on equilibrium parameters (3).

The fate of chromium in soils has been extensively studied (4). Chromium is derived from both anthropogenic and natural sources, and is mainly present in two stable oxidation states, (III) or (VI). Since Cr(VI) is mobile and more toxic than Cr(III), it is of great environmental concern. Chromium can be found naturally in water at concentrations up to 10 μg L⁻¹ (5). Contaminated sites can contain chromium at much higher concentrations. For instance, at the United Chrome Products site in Corvallis, Oregon, hexavalent chromium was measured at 280 mM in groundwater and 500 mM in soil near a leaking tank used to dispose of floor drippings, washings, and product rinsates (6). Another example is the old chromite ore refinement plant located in Jersey City, NJ. This abandoned site contains about 300,000 tons of chromium wastes buried beneath the facility, according to legal and environmental experts. Manganese oxides, which are common in soils, are strong oxidizing agents and can oxidize Cr(III) to Cr(VI). A number of previous studies have investigated chromium oxidation on manganese oxides employing batch techniques (7–13), X-ray photoelectron spectroscopy (XPS), transmission electron microscopy (TEM) (14, 15), and X-ray absorption fine structure (XAFS) studies (16, 17). The influence of bacteria on the oxidation rates (18) and modeling approaches (19, 20) have also been employed. However, there have been no studies focusing on the “chemical” kinetics of Cr(III) oxidation on manganese oxides, i.e., the initial rates of the reaction where mass transfer phenomena are negligible. This is mainly due to the lack of experimental techniques with data acquisition fast enough to follow rapid reactions. Recent advances in the use of real-time kinetic methodologies, particularly at the molecular scale, such as Quick XAFS (Q-XAFS) (21, 22) and attenuated total reflectance (ATR) Fourier transform infrared (FTIR) spectroscopy (23), as well as second harmonic generation (24), are promising tools for measuring rapid geochemical reactions.

Q-XAFS employs an ellipsoidal driving system that moves the monochromator in a fast cyclic motion, up and down in energy (25). Consequently, one can successively and rapidly take several scans within a couple of seconds, which contrasts with “regular” XAFS where the scan acquisition time is on the order of minutes. Our current Q-XAFS setup collects a scan each 0.75 s, which is less than the 1 min scanning time reported in the study of 22 which is, to our knowledge, along with 21, the only application of Q-XAFS to the study of an environmental mineral/water system.

With Q-XAFS, one can notably follow rapid oxidation state changes by analyzing the X-ray absorption near-edge structure (XANES) portion of the spectrum and rapid speciation changes by investigating the extended X-ray absorption fine structure (EXAFS) portion of the spectrum. In this study, the XANES region was analyzed to determine the rapid, initial oxidation of Cr(III) on hydrous manganese(IV) oxide (HMO), using Q-XAFS.

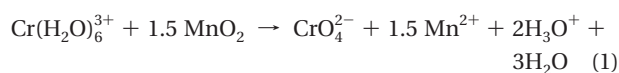
Materials and Methods

Chromium Solutions, Concentrations, and pH Range. All reagents and acids were ACS grade or better. Cr(III) stock

* Corresponding author.

solutions were prepared from chromium nitrate $\text{Cr}(\text{NO}_3)_3$ a few hours before conducting our experiments to minimize the effect of polymerization (26). $\text{Cr}(\text{VI})$ stock solutions were prepared from potassium chromate K_2CrO_4 . Distilled deionized water (Barnstead) with a resistivity of 18.2 M Ω was used to prepare all solutions. Q-XAFS experiments and batch experiments were performed using a $\text{Cr}(\text{III})$ concentration range of 40–100 mM, and at three different pH values, pH 2.5, pH 3, and pH 3.5. The synthesis and characterization of hydrous manganese oxide (HMO) are described in the Supporting Information (SI). The HMO suspension density was 20 g/L (230 mM MnO_2).

pH Control. To counter the pH drop at the beginning of the reaction due to the $\text{Cr}(\text{III})$ stock solution acidity, an adequate quantity of 4 M KOH to attain the pH of the experiment (pH 2.5, 3, or 3.5) was manually added to the manganese oxide solution, along with $\text{Cr}(\text{III})$. This amount of base was less than 1% of the total volume. The H^+ production from the $\text{Cr}(\text{III})$ oxidation (eq 1), which resulted in a constant decrease in pH throughout the reaction, was controlled by a pH Stat (Metrohm Titrimo) supplying 1 M KOH, at a maximum rate of 1 mL/min, and at a minimum rate of 25 $\mu\text{L}/\text{min}$ pH was controlled within ± 0.1 pH unit over a 30 min period.



Reaction Conditions. The range of chromium concentrations used in this study (40–100 mM), while high, can occur in chromium-contaminated sites (6). Our goal in this study was to measure chemical rate constants, determined from initial rate measurements using Q-XAFS, for $\text{Cr}(\text{III})$ oxidation by manganese oxide. Such constants are dependent only upon temperature, according to the Arrhenius equation, and not upon concentration (27). The lowest chromium concentration that could be used in this study was imposed by the Q-XAFS detection limit, which was experimentally measured at 30 ± 5 mM. This value represents the lowest concentration that can be employed to quantify the small $\text{Cr}(\text{VI})$ pre-edge feature appearing in the XANES spectra during the very first seconds of the $\text{Cr}(\text{III})$ oxidation reaction. A maximum chromium concentration of 100 mM implied to conduct our experiments below pH = 3.5 to avoid $\text{Cr}(\text{III})$ bulk precipitation, due to the low solubility of chromium (28). Consequently, all our experiments were conducted at pH 2.5, 3, and 3.5. Different hexavalent chromium remediation techniques employ synthetic reagents, for example, citric acid (29) or natural reagents, e.g., acid mine drainage (30). These leaching procedures are mostly efficient when applied at very low pH. Therefore, the rate parameters of $\text{Cr}(\text{III})$ oxidation reported in this study could be employed to assess the fate and effect of chromium in highly Cr contaminated sites where leaching procedures are applied at very low pH values. In these cases, although $\text{Cr}(\text{VI})$ is remediated and reduced to $\text{Cr}(\text{III})$, oxidation of $\text{Cr}(\text{III})$ may also occur, since manganese oxides are widespread in the environment (31).

The HMO suspension densities used in the traditional batch experiment and the batch Q-XAFS experiments were chosen based on the chromium concentration range and eq 1. According to eq 1, the oxidation of $\text{Cr}(\text{III})$ implies that 1 mol of $\text{Cr}(\text{III})$ reacts with 1.5 mol of HMO. Therefore, knowing that the maximum $\text{Cr}(\text{III})$ concentration that could be employed was 100 mM, and since we wanted to ensure that oxidation was not limited by the amount of Mn oxide present, 20 g/L of HMO was chosen as the suspension density.

Batch Kinetics Studies. HMO (13.85 mL of 26 g/L) was introduced into a polypropylene tube that was used as a batch vessel. Concentrated KOH (140, 220, and 300 μL) and

2.11, 2.03, and 1.95 mL of deionized water were added to the tubes for the experiments conducted at pH 2.5, 3, and 3.5, respectively. The total volume in each tube was 16.1 mL. An overhead stirrer promoted mixing inside the batch vessel. At $t = 0$, 1.9 mL of 0.95 M $\text{Cr}(\text{III})$ stock solution was added to the tubes. Thus, the final HMO suspension density was 20 g/L, and the chromium concentration was 100 mM. During the 45 min of reaction, 500 μL aliquots were collected at different time intervals with a 1-mL syringe and filtered using a 0.22- μm nylon filter. Each experiment was conducted in duplicate. The measurements of $\text{Cr}(\text{III})$, $\text{Cr}(\text{VI})$, and $\text{Mn}_{\text{aqueous}}$ concentrations are described in the SI.

Q-XAFS Experiments. The Q-XAFS experiments were performed at beamline X18B, National Synchrotron Light Source, Brookhaven National Laboratory, Upton, NY. The data acquisition method collects 60,000 points/30 seconds using a Keithley current amplifier, a sixteen-channel VME analog-digital-converter (ADC), and custom programmed Linux based software. The Bragg angle of a Si(111) double crystal monochromator is controlled via an assembly containing a microstepping motor, a rotating cam, and a small brass lever arm directly attached to the monochromator tangent arm (21, 25). The monochromator was set at the B3 position (5900–6363 eV), to obtain the XANES portion of the Cr spectrum. The beam was detuned at 30% from its maximum I_0 value. A gas mixture of 20% N_2 and 80% He was used in I_0 , and 100% N_2 was used in I_t to collect transmission data for the chromium foil, and fluorescence emission was collected with a PIPS detector. The monochromator motor setup allowed us to collect a scan every 0.75 s.

Experimental Setup. The batch experiments performed at beamline X18B were carried out using experimental conditions similar to those previously described. The same concentrations/quantity of reactants and same batch vessel were used. The batch vessel used for the Q-XAFS experiments featured ~ 1 cm above the bottom of the vessel, i.e., above the level of the stir bar, a rectangular hole window (1–3 cm) covered with kapton tape on the tube's wall so that the beam could pass through the tube and fluorescence could be emitted and detected with a fluorescence detector, and a stirrer was used to minimize mass transfer phenomena. One end of the tubing, containing the $\text{Cr}(\text{III})$ stock solution, was connected to the top inlet of the batch vessel with the other end of the tubing attached to a syringe placed outside the hutch. When the tube containing the manganese oxide solution, the fluorescence detector, the $\text{Cr}(\text{III})$ tubing, and the electrode of the pH stat were finally set at their respective position, the hutch was closed and quick scanning was initiated. After one minute of data collection, the $\text{Cr}(\text{III})$ stock solution was remotely injected inside the batch vessel via the syringe outside the hutch.

Although both $\text{Cr}(\text{VI})$ and $\text{Cr}(\text{III})$ possess a pre-edge feature in their respective XAFS spectrum, the $\text{Cr}(\text{VI})$ pre-edge feature at 5993.5 eV is prominent, and it is directly related to the proportion of $\text{Cr}(\text{VI})$ in the system. Therefore, one just has to measure the height of the pre-edge feature and compare it to a set of $\text{Cr}(\text{III})/\text{Cr}(\text{VI})$ mixtures to determine the quantity of $\text{Cr}(\text{VI})$ present in the system within a 1–5% error margin (17). Before conducting the kinetic experiments, XANES spectra for standard solution mixtures of 100 mM $[\text{chromium}]_{\text{totalCr(III)+Cr(VI)}}$ were collected and are shown in Figure S2.

Calculation of Initial Rates and Rate Constants. The reaction expression for $\text{Cr}(\text{III})$ oxidation by HMO is an equilibrium reaction (see eq 1). The overall rate equation contains both forward and backward reactions. However, if one measures the reaction kinetics at an early stage, only the forward reaction needs to be considered (3). In this case, the rate equation is reduced to:

$$\frac{d[\text{Cr(VI)}]}{dt} = k[\text{Cr(III)}]^\alpha [\text{MnO}_2]^\beta \quad (2)$$

where k is the rate constant in sec^{-1} , and α and β are the partial rate coefficients. Another simplification can be made by successively applying a large excess of one of the reactants and varying the concentration of the other reactant (isolation method). One thus would end up getting an even more simplified rate equation, since the reactant in large excess would be considered constant throughout the reaction and thus would not appear in the rate equation expression. An overall reaction order would then be assumed, and the integrated rate law equation would be applied with the $[\text{Cr(VI)}]$ experimental values. If a linear trend resulted, the assumed rate order would be validated.

However, the isolation method could not be applied in this study because of the inability to have a large excess of one of the reactants. With our particular system, the Cr(III) concentration could not be increased to more than 100 mM due to solubility factors, and could not be decreased below 30 mM because of the Q-XAFS detection limit. Similarly, increasing the HMO suspension density above 30 g/L would have resulted in a high suspension viscosity, which would have complicated the stirred batch experiments. Decreasing the HMO concentration to a much lower value was also not possible, since a small amount of HMO would have resulted in a small amount of Cr(VI) produced, and thus the quantification of Cr(VI) at early stages of the reaction would have been compromised.

Consequently, the initial rate method was applied to determine the rate parameters for the oxidation reaction rather than the isolation method. With this approach, one of the reactants is fixed at a constant value (but not necessarily in excess) in a set of experiments, while the concentration of the other reactant is successively varied. Therefore, both of the reactants must be considered in the overall rate equation. During the early stage of the reaction, a linear relationship relates $[\text{Cr(VI)}]$ and time. The slope of this linear trend is the initial rate i , which is defined as:

$$\frac{d[\text{Cr(VI)}]}{dt} = k[\text{Cr(III)}]_0^\alpha [\text{MnO}_2]_0^\beta = i \quad (3)$$

where k , α , and β were defined earlier, 0 represents the initial concentrations, and i is the initial rate of the reaction. To measure the partial rate coefficient of chromium α at a given pH value for the experiments where $[\text{MnO}_2]$ was fixed and $[\text{Cr(III)}]$ was varied, eq 6 was used, which is a simplified expression of eq 4:

$$\frac{i_{\text{exp1}}}{i_{\text{exp2}}} = \frac{k[\text{Cr(III)}_{\text{exp1}}]^\alpha [\text{MnO}_{2\text{fixed}}]^\beta}{k[\text{Cr(III)}_{\text{exp2}}]^\alpha [\text{MnO}_{2\text{fixed}}]^\beta} \quad (4)$$

where exp = experiment.

Hence:

$$\frac{i_{\text{exp1}}}{i_{\text{exp2}}} = \left(\frac{[\text{Cr(III)}_{\text{exp1}}]}{[\text{Cr(III)}_{\text{exp2}}]} \right)^\alpha \quad (5)$$

Therefore:

$$\alpha = \frac{\log\left(\frac{i_{\text{exp1}}}{i_{\text{exp2}}}\right)}{\log\left(\frac{[\text{Cr(III)}_{\text{exp1}}]}{[\text{Cr(III)}_{\text{exp2}}]}\right)} \quad (6)$$

To measure the partial rate coefficient of manganese β at a given pH value for the experiments where $[\text{Cr(III)}]$ was fixed and $[\text{MnO}_2]$ was varied, eq 9 was used, which is a simplification of eq 7:

$$\frac{i_{\text{exp3}}}{i_{\text{exp4}}} = \frac{k[\text{Cr(III)}_{\text{fixed}}]^\alpha [\text{MnO}_{2\text{exp3}}]^\beta}{k[\text{Cr(III)}_{\text{fixed}}]^\alpha [\text{MnO}_{2\text{exp4}}]^\beta} \quad (7)$$

Thus:

$$\frac{i_{\text{exp3}}}{i_{\text{exp4}}} = \left(\frac{[\text{MnO}_{2\text{exp3}}]}{[\text{MnO}_{2\text{exp4}}]} \right)^\beta \quad (8)$$

Therefore:

$$\beta = \frac{\log\left(\frac{i_{\text{exp3}}}{i_{\text{exp4}}}\right)}{\log\left(\frac{[\text{MnO}_{2\text{exp3}}]}{[\text{MnO}_{2\text{exp4}}]}\right)} \quad (9)$$

The rate constant k was calculated for each experiment using the i values experimentally measured, and the β and α calculated for each pH value, using eq 10, which is a rearrangement of eq 3:

$$k = \frac{i}{[\text{Cr(III)}]^\alpha [\text{MnO}_2]^\beta} \quad (10)$$

Although initial rate methods are more difficult to perform than isolation methods since i must be measured in a very short time period, the Q-XAFS technique was able to collect enough data points at the beginning of the reaction to determine initial rates (Figure 3).

Results and Discussion

Traditional Batch Kinetic Experiments. The results of the batch experiments conducted at pH 2.5, 3, and 3.5, are depicted in Figure 1a, b, and c, respectively. The lower the pH, the more the reaction (eq 1) is shifted toward the products, i.e. more Cr(VI) and aqueous Mn are present in solution at pH 2.5 than at pH 3.5 (Figure 1). Stirred flow experiments, to test if the manganese oxide dissolves in acidic medium, showed no manganese dissolution from the HMO, for the three different pH values (data not shown). Consequently, the high manganese production obtained during our batch experiments and depicted in Figure 1 is derived from the oxidation of chromium on the manganese oxide surface, rather than HMO dissolution due to the acidic medium. The sum of aqueous Cr(III) and Cr(VI) for each aliquot, at each pH value, is lower than 100 mM, meaning that chromium is sorbed on HMO. This amount increases with reaction time and pH value. At pH 3.5, about 12 mM of Cr(VI) is present in solution after 45 min, whereas about ~18 mM is present in solution at pH 3 after 45 min, and ~35 mM is present at pH 2.5. Lower values of dissolved $\text{Cr(VI)}_{\text{aqueous}}$ at pH 3.5 compared to lower pH values is not due to more chromate anions being retained on HMO, since the mineral surface is negatively charged at pH 3.5 (PZC 2.7 for HMO). Consequently, lower $\text{Cr(VI)}_{\text{aqueous}}$ concentration with increasing pH suggests lower Cr(III) oxidation rates. The formation of a chromium hydroxide precipitate on the surface of the manganese oxide may be responsible for the low Cr(III) oxidation rates at pH 3.5 and the higher amount of chromium sorbed at this pH compared to lower pH values, since Cr(III) starts to precipitate close to pH 3.5 at the chromium concentration used in the experiment (28). This precipitate could both reduce the amount of available Cr(III) to react with the HMO, and shield the mineral surface, preventing further Cr(III) sorption and thus oxidation (14). The formation of a chromium hydroxide surface precipitate was reported on the surface of birnessite, which belongs to the hexagonal birnessite family, like HMO (32).

Q-XAFS Experiments. Data collected from a typical Q-XAFS batch experiment conducted at pH = 2.5 is depicted in Figure 2. The growth of the XANES pre-edge feature at

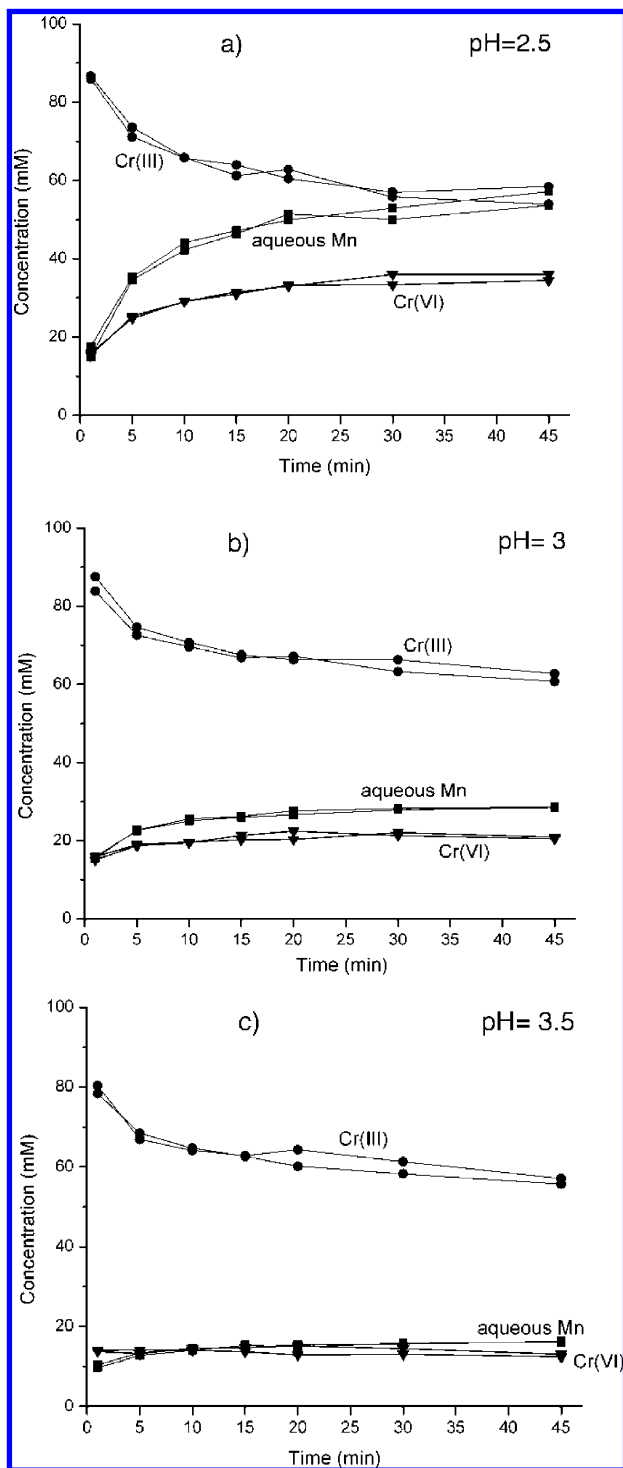


FIGURE 1. Kinetics of Cr(III) oxidation on HMO at (a) pH 2.5, (b) pH 3, and (c) pH 3.5, using a batch technique and reaction conditions of 100 mM Cr(III) and 20 g/L HMO.

5993.5 eV demonstrates that Cr(VI) is produced in the batch vessel as time proceeds. Cr(III) oxidation is particularly rapid during the first 120 s of the reaction, when about 35 mM of chromate is produced, followed by a slower rate. This biphasic trend taking place within the first 4 min was not only observed for the experiment shown in Figure 2, but also for all experiments carried out in this study to measure the rates of Cr(III) oxidation.

After 240 s (4 min) of the experiment shown in Figure 2, 30 mM of Cr(VI) was produced (Figure S3), which represents 30% of [Cr(III)] initially introduced. At the same experimental conditions, about 25 mM was measured with the traditional

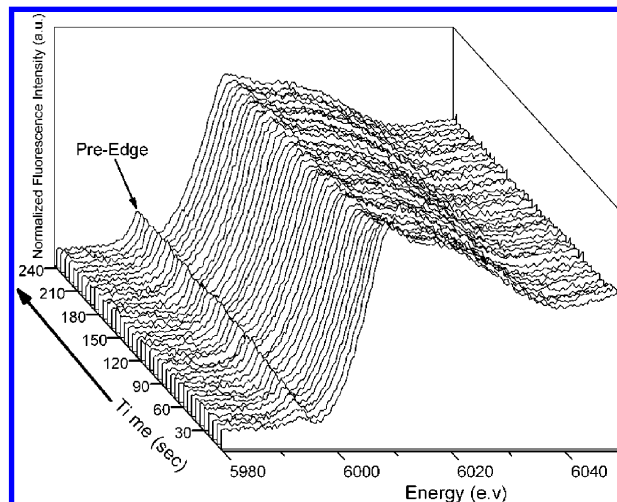


FIGURE 2. Cr(III) oxidation kinetics using a Q-XAFS technique, at pH 2.5, [Cr(III)] = 100 mM, [HMO] = 20 g/L, and 0–240 s. Each XANES spectrum shown represents 3 s of the reaction (average of four 0.75 s spectra).

batch method. The latter experimental approach only measures aqueous Cr(VI), and not the total amount of Cr(VI), i.e., aqueous Cr(VI) and chromate sorbed on the manganese oxide, while the Q-XAFS experiment measures both aqueous and sorbed chromate. The higher Cr(VI) concentration measured with batch Q-XAFS compared to the traditional batch kinetic method at the same reaction times suggests that some chromate is sorbed on the surface of HMO at pH 2.5. To obtain further evidence that Cr(VI) is present on the manganese oxide surface, traditional batch experiments with the same experimental conditions were carried out near beamline X18B in a laboratory at the NSLS. Aliquots were taken out at different time intervals (1, 5, 10, 15, 20, 30, and 45 min) and filtered with a 0.22- μ m filter. Manganese oxide pastes were analyzed immediately with bulk X-ray absorption spectroscopy to measure the ratio of Cr(VI) to Cr(III) in the pastes (Figure S4), by calculating the height of the pre-edge feature at 5993.5 eV. Figure S4 shows that at pH 2.5 and a 1 min reaction time, 87% of the chromium was Cr(VI), suggesting that chromate is sorbed on the manganese oxide. This proves that using a Q-XAFS batch method to measure the rates for Cr(III) oxidation with HMO at these experimental conditions is more appropriate than a traditional batch kinetic method since the entire amount of Cr(VI) produced from the chromium oxidation is measured, including the amount sorbed on the manganese oxide.

A series of Q-XAFS batch experiments were carried out with different reactant concentrations and pH values to measure rate parameters for the Cr(III) oxidation by HMO (Table 1). The duplicate values for each experiment are very close to each other, meaning that the reproducibility of the Q-XAFS method is acceptable. To obtain the experimental initial rates, Cr(VI) was quantified from the pre-edge feature height for each experiment during a time period between time zero and the first minute of the reaction. When [Cr(VI)] was plotted over the first 6 s of the reaction, a straight line resulted. The initial rate is equal to the slope (3). The uncertainty in our measurements is given by the standard error of the slope, and was found to be low for most measured initial rates (Table 1). As an example, a plot of one initial rate measurement is depicted in Figure 3. For all experiments conducted at different Cr(III) concentrations (from 40 to 100 mM) and HMO suspension density (from 5 to 20 g/L), the first data point was measured at 1.5 s (average of two 0.75 scans). Data points collected after 6 ± 1.5 s resulted in a decrease of the R^2 (quality of the slope). Therefore, the initial rate was measured between 1.5 and 6 ± 1.5 s for all

TABLE 1. Initial Conditions, Measured Initial Rates, and Rate Parameters^a

[Cr(III)] (mM)	[HMO] (g/L)	initial rates (mol/L/sec)			k (sec ⁻¹)		
		pH = 2.5	pH = 3	pH = 3.5	pH = 2.5	pH = 3	pH = 3.5
100	20	0.0045/0.0052 <i>(0.00036/0.00071)</i>	0.0045/0.0045 <i>(0.00067/0.00064)</i>	0.0045/0.0047 <i>(0.0004/0.0006)</i>	0.204/0.228	0.277/0.202	0.295/0.364
80	20	0.0035/0.0040 <i>(0.00017/0.00021)</i>	0.0034/0.0035 <i>(0.00031/0.00066)</i>	0.0039/0.0030 <i>(0.00108/0.00046)</i>	0.202/0.220	0.270/0.198	0.353/0.308
60	20	0.0025/0.0029 <i>(0.0002/0.00037)</i>	0.0027/0.0028 <i>(0.0004/0.00017)</i>	0.0022/0.0022 <i>(0.00043/0.00034)</i>	0.197/0.215	0.303/0.208	0.302/0.357
40	20	0.0017/0.0021 <i>(0.00023/0.00003)</i>	0.0015/0.0018 <i>(0.00028/0.00034)</i>	0.0012/0.0012 <i>(0.00017/0.00017)</i>	0.208/0.235	0.266/0.199	0.296/0.363
<i>Cr partial rate coefficient α</i>							
		1.08/1.01 1.09	1.13/1.05 1.09	1.43/1.53 1.48			
100	20	0.0045/0.0052 <i>(0.00036/0.00071)</i>	0.0045/0.0045 <i>(0.00067/0.00064)</i>	0.0045/0.0047 <i>(0.0004/0.0006)</i>	0.204/0.228	0.277/0.202	0.295/0.364
100	15	0.0035/0.0036 <i>(0.0006/0.0005)</i>	0.0035/0.0036 <i>(0.00046/0.00052)</i>	0.0037/0.0038 <i>(0.00032/0.00054)</i>	0.206/0.207	0.293/0.219	0.291/0.328
100	10	0.002/0.002 <i>(0.00039/0.00039)</i>	0.0023/0.0020 <i>(0.0001/0.00021)</i>	0.0028/0.0029 <i>(0.0008/0.00059)</i>	0.169/0.171	0.287/0.244	0.280/0.311
100	5	0.001/0.0012 <i>(0.00039/0.00001)</i>	0.0010/0.0014 <i>(0.0001/0.0001)</i>	0.0020/0.0022 <i>(0.00035/0.00031)</i>	0.157/0.203	0.257/0.316	0.283/0.346
<i>Mn partial rate coefficient a</i>							
		0.90/0.98 0.94	1.00/1.05 1.02	0.58/0.53 0.55			
<i>k (averaged) in sec⁻¹</i>							
		pH = 2.5 0.192/0.211 0.201	pH = 3 0.279/0.227 0.242	pH = 3.5 0.300/0.340 0.322			

^a The partial rate coefficients α , β at pH 2.5, pH 3, and pH 3.5 shown in this table are averaged values from α and β calculated using eqs 6 and 9 and by combining the initial rates measured at different experimental conditions. The rate constant for each experiment was measured with eq 10. Since all experiments were duplicated, the initial rates and rate parameters are reported with two values separated with "/". The standard error (95% confidence interval) for each initial rate is italicized. Averages of duplicate values are highlighted in bold.

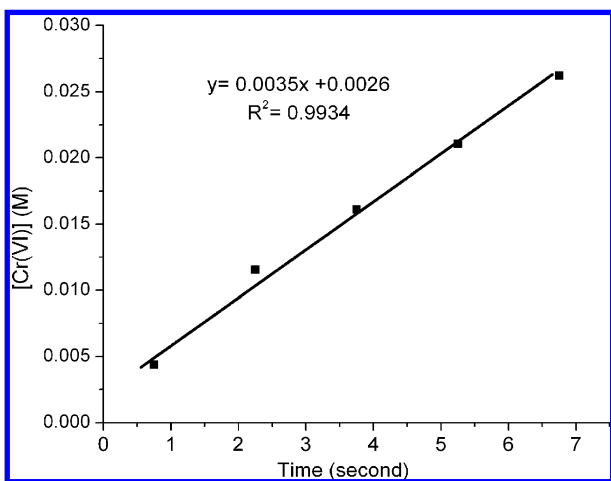


FIGURE 3. Initial rate measurement for an experiment at pH 2.5, where [Cr(III)] = 80 mM, and [HMO] = 20 g/L.

experiments, which represents 4 ± 1 data points. The R^2 of the slope for all experiments was ≥ 0.96 .

After getting the i values for each experiment, we determined the partial rate coefficients α , β (shown in eq 2), and the rate constants. A summary of the initial concentrations, the initial rates measured experimentally (i), and the rates parameters (α , β , and k) for all experiments are summarized in Table 1.

The rate parameters from Table 1 inserted in eq 2 give these following rate equations:

$$\text{pH 2.5} \quad \frac{d\text{Cr(VI)}}{dt} = k[\text{Cr}^{3+}]^{1.04}[\text{MnO}_2]^{0.94} \quad k = 0.201 \text{ s}^{-1} \quad (11)$$

$$\text{pH 3} \quad \frac{d\text{Cr(VI)}}{dt} = k[\text{Cr}^{3+}]^{1.08}[\text{MnO}_2]^{1.03} \quad k = 0.242 \text{ s}^{-1} \quad (12)$$

$$\text{pH 3.5} \quad \frac{d\text{Cr(VI)}}{dt} = k[\text{Cr}^{3+}]^{1.48}[\text{MnO}_2]^{0.56} \quad k = 0.322 \text{ s}^{-1} \quad (13)$$

The partial rate coefficients reported in eqs 11, 12, and 13 show that a variation in the pH by a half unit changes the way the two reactants affect the kinetics of the reaction. These results were expected, since more Cr(III) and Mn(IV) are likely to react together when the mineral surface becomes more negatively charged at higher pH values (PZC of HMO = 2.7). The increase in the rate constant k from pH 2.5 to pH 3.5 also confirms our expectations. At the early stage of the reaction, the higher the pH, the higher the rate of Cr(III) oxidation (8). However, increasing the pH reduces the solubility of chromium. It may precipitate at the surface of the manganese oxide in a chromium hydroxide surface precipitate, even when the chromium concentration is below its saturation index (16). Therefore, it has been postulated that although the initial oxidation rate is higher at high pH at the beginning of the reaction, chromium oxidation shuts down rapidly at high pH, likely due to the build up of a surface precipitate that impedes further interactions between Cr(III) and the manganese oxide surface. This surface precipitate formation was observed with birnessite for experimental conditions of pH 3.5 and a Cr^{3+} concentration of 770 μM (14). These results suggest that one could divide the oxidation into two time periods: a first period during which only chromium and the HMO surface interact with each other, and a second period during which a chromium hydroxide surface precipitate forms and can influence the rates of Cr(III) oxidation. However, the kinetics of formation of the surface

precipitate, as well as its exact nature, are still unknown. These particular topics will be addressed in a future study.

Although a few studies have reported rates of Cr(III) oxidation on manganese oxides, comparing previous results and rate parameters to those reported in this study are difficult, because of the many differences in experimental conditions. The rate constants of trivalent chromium oxidation with MnO₂ notably depend on temperature, Cr(III) concentration and pH (8), the manganese oxide suspension density and nature (11), the kinetic equation considered (since it defines the rate constant unit), and the time scale at which the kinetic parameters are being measured (chemical rate constants versus apparent rate constants). For example, Johnson and Xyla (13) reported *k* values for Cr(III) oxidation with manganite (γ -MnOOH). Their rate constants (in L m⁻² s⁻¹) were measured on several minutes (compared to a few seconds in our study), at pH between 3.5 and 9.5, and at a range of Cr(III) concentration of 0.25–5 μ M (compared to 40–100 mM in our study). Therefore, it would be difficult to compare their kinetic parameters with our results, since too many factors influence Cr(III) oxidation. Another study (33) reported rate constants for Cr(III) oxidation on acid birnessite measured over 30 min using a batch technique, at 50 μ M Cr(III), 0.1 g/L of acid birnessite, and pH 3, 4, 5, and 6. The rate constant at pH 3 was equal to 0.0018 s⁻¹, and was 0.005 s⁻¹ at pH 4. Therefore, the rate constant at pH 3 reported in this previous study is much lower than the rate constant measured at pH 3 in the present study, which is probably due to the differences in experimental conditions and the time scale at which those rates were measured. The Arrhenius equation states that the chemical rate constant *k* is only dependent upon temperature, and not upon concentration or mixing speed. One sees from Table 1 that the *k* values are similar for all experiments carried out at a given pH and for different Cr(III) and manganese oxide concentrations. The same mixing speed value was used throughout this study: ~240 rotations per minute in the batch vessel. The experiment at pH 2.5 and 80 mM Cr(III) was repeated several times and the mixing speed was increased by a factor of 0.2, 0.5, and 1 order of magnitude. The same *k* value was obtained, regardless of the mixing speed (data not shown). Therefore, Cr(III) concentration, HMO suspension density, pH, and mixing speed did not affect the rate constants measured with quick XAFS. This further strengthens our argument that chemical reaction rates were measured in this study.

Acknowledgments

We thank Ryan Tappero, Syed Khalid, Ivan So, and Nebojsa Marinkovic for their assistance during Q-XAFS data collection; Nathan Hould and Jonathon Hanson for assistance in Q-XAFS data reduction; and the three anonymous reviewers for their inputs that considerably improved the content of this manuscript.

Supporting Information Available

Chromium pre-edge height calibration curve, HMO XRD pattern, and additional XANES spectra of experiments taken at different reaction times and experimental conditions (pH, chromium, and manganese oxide concentrations). This material is available free of charge via the Internet at <http://pubs.acs.org/>.

Literature Cited

- (1) Amacher, M. C. Methods of Obtaining and Analyzing Kinetic Data. In *Rates of Soil Chemical Processes*, Sparks, D. L., Suarez, D. L., Eds.; SSSA Spec. Publ. No. 27, 19–59; Soil Sci. Soc. Am.: Madison, WI, 1991.
- (2) Fendorf, S. E.; Sparks, D. L.; Camaioni, D. M. Electron paramagnetic resonance stopped flow kinetic study of manganese(II) sorption desorption on birnessite. *Soil Sci. Soc. Am. J.* **1993**, *57*, 57–62.

- (3) Sparks, D. L. *Kinetics of Soil Chemical Processes*; Academic Press: San Diego, CA, 1986.
- (4) Fendorf, S. E. Surface reactions of chromium in soils and waters. *Geoderma* **1995**, *67*, 55–71.
- (5) Dirilgen, N.; Dogan, F. Speciation of chromium in the presence of copper and zinc and their combined toxicity. *Ecotoxicol. Environ. Saf.* **2002**, *53* (3), 397–403.
- (6) Palmer, C.; Wittbrodt, P. Processes affecting the remediation of chromium-contaminated sites. *Environ. Health Perspect.* **1991**, *92*, 25–40.
- (7) Eary, E.; Rai, D. Kinetics of chromium(III) oxidation to chromium(VI) by reaction with manganese dioxide. *Environ. Sci. Technol.* **1987**, *21*, 1187–1193.
- (8) Fendorf, S. E.; Zasoski, R. J. Chromium(III) oxidation by δ -MnO₂. 1. Characterization. *Environ. Sci. Technol.* **1992**, *26*, 79–85.
- (9) Kim, J. G.; Moon, H.-S. Oxidation of chromium (III) to chromium (VI) by a series of synthesized birnessites (δ -MnO₂): kinetics and oxidation capacity. *Clay Miner.* **1998**, *10*, 363–374.
- (10) Kim, J. G.; Dixon, J.; Chusui, C. C.; Deng, Y. Oxidation of chromium(III) to (VI) by manganese oxides. *Soil Sci. Soc. Am. J.* **2002**, *66*, 306–316.
- (11) Weaver, R. M.; Hochella, M. F. The reactivity of seven Mn-Oxides with Cr³⁺_{aq}: a comparative analysis of a complex, environmentally important redox reaction. *Am. Mineral.* **2003**, *88*, 2016–2028.
- (12) Stepniewska, Z.; Bucior, K.; Benucci, R. P. The effects of MnO₂ on sorption and oxidation of Cr(III) by soils. *Geoderma* **2004**, *122*, 291–296.
- (13) Johnson, A. C.; Xyla, A. G. The oxidation of chromium(III) to chromium(VI) on the surface of Manganite (γ -MnOOH). *Geochim. Cosmochim. Acta* **1991**, *55*, 2861–2866.
- (14) Fendorf, S. E.; Fendorf, M.; Sparks, D. Inhibitory mechanisms of Cr(III) oxidation by δ -MnO₂. *J. Colloid Interface Sci.* **1992**, *153* (1), 37–54.
- (15) Banerjee, D.; Nesbitt, H. W. Oxidation of aqueous Cr(III) at birnessite surfaces: constraints on reaction mechanism. *Geochim. Cosmochim. Acta* **1999**, *63* (11/12), 1671–1687.
- (16) Manceau, A.; Charlet, L. X-ray adsorption spectroscopy study of the sorption of Cr(III) at the oxide-water interface. I. Molecular mechanism of Cr(III) oxidation on Mn Oxides. *J. Colloid Interface Sci.* **1992**, *148*, 425–442.
- (17) Peterson, M. L.; Brown, G. E.; Parks, G. A.; Stein, C. L. Differential redox and sorption of Cr(III/VI) on natural silicate and oxide minerals: EXAFS and XANES results. *Geochim. Cosmochim. Acta* **1997**, *61* (16), 3399–4413.
- (18) Murray, K.; Tebo, B. Cr(III) is indirectly oxidized by the Mn(II)-oxidizing bacterium bacillus sp. Strain SG-1. *Environ. Sci. Technol.* **2007**, *41*, 528–533.
- (19) Guha, H.; Saiers, J.; Brooks, S.; Jardine, P.; Jayachandran, K. Chromium transport, oxidation, and adsorption in manganese-coated sand. *J. Contam. Hydrol.* **2001**, *311*–334.
- (20) Lin, C.-J. The chemical transformations of chromium in natural waters - A model study. *Water, Air Soil Pollut.* **2002**, *139* (137–158), 137.
- (21) Ginder-Vogel, M.; Landrot, G.; Fischel, J.; Sparks, D. L. Quantification of rapid environmental redox processes using quick scanning x-ray absorption spectroscopy (Q-XAS). *Proc. Natl. Acad. Sci. U.S.A.* **2009**, *106* (38), 16124–16128.
- (22) Mitsunobu, S.; Takahashi, Y.; Uruga, T. Observation of chemical reactions at the solid-water interface by Quick XAFS combined with a column reactor. *Anal. Chem.* **2005**, *78*, 7040–7043.
- (23) Parikh, S. J.; Lafferty, B. J.; Sparks, D. L. An ATR-FTIR spectroscopic approach for measuring rapid kinetics at the mineral/water interface. *J. Colloid Interface Sci.* **2008**, *320*, 177–185.
- (24) Mifflin, A.; Gerth, K.; Geizer, F. Kinetics of chromate adsorption and desorption at fused quartz/water interfaces studied by second harmonic generation. *J. Phys. Chem. A* **2003**, *107*, 9620–9627.
- (25) Dent, A. J. Development of time-resolved XAFS instrumentation for quick EXAFS and energy-dispersive EXAFS measurements on catalyst systems. *Top. Catal.* **2002**, *18* (1–2), 27–35.
- (26) Rotzinger, F.; Stünzi, H.; Marty, W. Early stages of the hydrolysis of chromium(III) in aqueous solution. 3. Kinetics of dimerization of the deprotonated aqua ion. *Inorg. Chem.* **1986**, *25*, 489–495.
- (27) Sparks, D. L. *Environmental Soil Chemistry*; Academic Press: San Diego, CA, 2003.
- (28) Rai, D.; Sass, B.; Moore, D. Chromium(III) hydrolysis constants and solubility of chromium(III) hydroxide. *Inorg. Chem.* **1987**, *26*, 345–349.
- (29) Yang, J. W.; Tang, Z. S.; Guo, R. F.; Chen, S. Q. Soil surface catalysis of Cr(VI) reduction by citric acid. *Environ. Prog.* **2008**, *27* (3), 302–307.

- (30) Kingston, S. H. M.; Cain, R.; Huo, D.; Rahman, M. G. M. Determination and evaluation of hexavalent chromium in power plant coal combustion by-products and cost-effective environmental remediation solutions using acid mine drainage. *J. Environ. Monit.* **2005**, *7*, 899–905.
- (31) Post, J. E. Manganese oxide minerals: crystal structures and economic and environmental significance. *Proc. Natl. Acad. Sci.* **1999**, 3447–3454.
- (32) Villalobos, M.; Toner, B.; Bargar, J.; Sposito, G. Characterization of the manganese oxide produced by *Pseudomonas putida* strain MnB1. *Geochim. Cosmochim. Acta* **2003**, *67* (14), 2649–2662.
- (33) Nico, P.; Zasoski, R. Importance of Mn(III) availability on the rate of Cr(III) oxidation on δ MnO₂. *Environ. Sci. Technol.* **2000**, *34*, 3363–3367.

ES901759W